OPO OPHTHALMIC & PHYSIOLOGICAL OPTICS
THE JOURNAL OF THE COLLEGE OF OPTOMETRISTS

Ophthalmic & Physiological Optics ISSN 0275-5408

Influence of background on image recognition in normal vision and age-related macular degeneration

Cécile Bordier[1,2], Julie Petra[1,2], Catherine Dauxerre[1,2], François Vital-Durand[1,2] and Kenneth Knoblauch[1,2]

[1]INSERM, U846, Stem Cell and Brain Research Institute, Department of Integrative Neurosciences, Bron, France and [2]Université de Lyon, Lyon, France

Citation information: Bordier C, Petra J, Dauxerre C, Vital-Durand F & Knoblauch K. Influence of background on image recognition in normal vision and age-related macular degeneration. *Ophthalmic Physiol Opt* 2011, **31**, 203–215. doi: 10.1111/j.1475-1313.2011.00820.x

Keywords: age, age-related macular degeneration, eccentricity, image recognition, spatial frequency bandwidth

Correspondence: Cécile Bordier
E-mail address: cecile.bordier@ujf-grenoble.fr

Received: 25 August 2010; Accepted: 26 December 2010

Abstract

Purpose: The influence of background attenuation on the spatial frequency bandwidth requirements for image recognition was assessed in normal young and older groups and in a group with age-related macular degeneration (AMD). Bandwidth requirements were also assessed in the visual periphery of young normal observers.

Methods: In Experiment 1, each observer was presented with 20 series of images. Each series consisted of a sequence of progressively low-pass filtered images, presented in an order of increasing bandwidth, i.e., according to an ascending method of limits. For half of the series, the background of the base image was selectively darkened by 80% of its original luminance. Three measures were analyzed: (1) the critical bandwidth defined as the bandwidth in cycles/image (cpi) at which 50% of the images were recognized, (2) the minimal bandwidth, defined as the minimal bandwidth at which images were recognized and (3) the proportion of images recognized at full bandwidth. In Experiment 2, young normal observers were similarly tested in central vision and at 5.5° eccentricity (superior or inferior visual field). A third background attenuation condition was included, as well, in which the background was low-pass filtered.

Results: The critical bandwidth for image recognition was significantly reduced by darkening the image background for normal young and old and the AMD groups. This improvement was found to be contrast dependent for the darkened background. In addition, AMD observers tended to recognize more images at full bandwidth if the background was darkened. For normal young observers, making the background low-pass was ineffective in lowering the critical bandwidth in the fovea. Fewer images were recognized at full bandwidth at 5.5° eccentricity for a low-pass background and marginally fewer for a darkened background.

Conclusions: Selective attenuation of the image background can lead to reductions in the bandwidth requirements for image recognition in AMD. However, performance of young normal observers for images presented in the periphery was unlike AMD performance under the conditions investigated. These results have interesting implications for the design of image enhancement algorithms to aid low vision observers.

Introduction

Age-Related Macular Degeneration (AMD) is one of the principal causes of vision loss in industrialized nations for people over 65 years old.[1,2] AMD can be a debilitating pathology, resulting in a central visual field defect that entails visual acuity and contrast sensitivity losses. Visual performance on tasks necessary for daily living, such as reading,[3] writing and recognition of faces and objects,[4] is often severely impaired; in addition, the risk for falls is significantly increased.[5]

Current treatments attempt to stabilize the evolution of AMD,[6,7] but typically cannot restore full visual function. Indeed, there are several forms of AMD, not all of which are susceptible to the same treatments. Rehabilitation procedures aim at improving visual performance on daily living tasks.[8,9] Numerous approaches are under development, including re-training of fixation strategies to exploit retinal regions less affected by the pathology and the use of optical and opto-electronic devices to render text and images easier to process.[1–15] Much of the research has focussed specifically on characterizing and improving reading performance[16] although a few studies have considered other visual tasks.[4, 17–20]

Two recent studies suggest that object recognition performance is enhanced in AMD observers when contextual information is suppressed.[18,21] Mazoyer *et al.*[18] reported that patients with AMD required nearly twice as much bandwidth to recognize photographs of objects in a natural scene than for line drawings or images of isolated objects on a white background. It was hypothesized that the added bandwidth requirement for photographs reflected a deficit in figure/ground separation, possibly related to lower resolution[22] and greater contour interaction (or crowding)[23–25] in the peripheral visual field, the region of the visual field with which such patients are obliged to view the world. Boucart *et al.*[21] arrived at similar conclusions based on experiments that showed that AMD observers could classify images of isolated objects as animal or face more rapidly and more accurately than when presented with a context.

Potentially, these observations have important consequences for image processing approaches that seek to enhance images for low vision observers. Most techniques proposed treat the image uniformly, the same computations being performed over the whole image irrespective of whether a particular region corresponds to a part of the object or the background.[26] Thus, information attenuated (enhanced) from objects in the image is also attenuated (enhanced) from the background. A deficit of figure/ground processing, however, would suggest that selective attenuation of background information would be preferable to render images more easily recognized by AMD patients. Some recent image segmentation algorithms[27,28] and low vision devices incorporating them,[29,30] in fact, move in this direction.

Minimal (or critical) bandwidth for recognition has already provided a useful measure of performance and information processing on diverse tasks.[3,31–35] Our goal was to examine further the effect of background attenuation on the bandwidth for image recognition in macular pathology. Specifically, we sought to test if the bandwidth advantage for segmented images is specific to observers with AMD or if the phenomenon can also be demonstrated in the central vision of young and older observers. In addition, we tested whether this phenomenon is present in the normal peripheral visual field.

Methods

Observers

The research followed the tenets of the Declaration of Helsinki, and informed consent was obtained from all participants in the studies described herein. Two experiments were performed. In the first one, three groups were tested, normal young, normal aged and AMD observers. Thirteen normal young adults (mean age ± S.D.: 25.3 ± 3.2 years) and 20 older adults (mean age ± S.D.: 72.4 ± 7.7 years) comprised the two groups with normal central visual fields. Fourteen patients diagnosed with advanced bilateral AMD (mean age ± S.D.: 81.9 ± 5.4 years; age >60 years) also participated. The AMD patients' visual acuity in the best eye was inferior to 0.4 logMAR (mean acuity ± S.D.: 0.82 ± 0.3). Visual field alterations, scotoma and isopters were measured by Goldmann dynamic perimetry. Patients included presented with either neo-vascular or with atrophic AMD but no other causes of low visual acuity. The young groups were tested in the laboratory and the older and AMD groups in an ophthalmology office. Their summary characteristics are shown in *Table 1*. In four cases, the participating clinicians did not record the scotoma type and in two, the AMD type. These characteristics are noted as not available (NA). In the second experiment, 10 normal, young observers participated (mean age ± S.D.: 25.8 ± 4.5 years).

Stimuli

All stimuli were presented on a 21″ television monitor (Vision Master 502, Iiyama; http://www.iiyama.com/). The luminance/grey level relation was calibrated with a spectrophotometer (Minolta CS100) and characterized by adjusting the parameters k and γ to the calibration data by a least-squares fit of the equation

Table 1. Patient summary information

Patient ID	Eye tested	Acuity (logMAR)	Reading (words min^{-1})	Scotoma type	AMD type
1	R	1.0	0	Rel	NV
2	R	0.7	36	NA	AT
3	L	1.1	14	NA	NA
4	R	0.6	47	Rel	NV
5	L	0.4	54	NA	NA
6	R	0.4	113	Rel	AT
7	R	0.7	26	Abs	NV
8	R	1.0	0	Abs	NV
9	R	1.1	0	Abs	NV
10	L	0.6	30	Rel	NV
11	R	0.7	33	Abs	NV
12	L	1.3	24	Rel	NV
13	R	0.7	13	NA	AT
14	L	1.2	0	Abs	NV

NA, data not available; Scotoma type: Abs, absolute; Rel, relative; AMD type: NV, Neovascular; AT, Atrophic.

$$L(N) = L_0 + kN^{\gamma}, \tag{1}$$

where N is the gray level (0–255), L the measured luminance in candelas per meter^2 (cd m^{-2}) and L_0 the luminance at 0 grey level. Based on this expression, all image calculations were performed in the luminance domain and subsequently back-transformed into gray level for image display. The root mean square (rms) of the luminance distribution for each image was calculated by the formula

$$\text{rms} = \left(\frac{\sum_i (L_i - \bar{L})^2}{n} \right)^{\frac{1}{2}}, \tag{2}$$

where L_i is the luminance of the ith pixel, $\bar{L}$ the mean luminance across the image of n pixels and was used as a measure of global image contrast.

In the first experiment, 40 grey scale images (resolution: 256 × 256 pixels) were selected. The images were photographs, each with a prominent object in the foreground that was embedded in a background. The images were of varied subject matter: animals, plants, sport scenes, household objects, persons, etc. Four examples are shown in *Figure 1*. A second group of 40 images was generated from the original set in which the background luminance was selectively reduced (or darkened, see *Figure 2b*), in order to render its details less salient and to

Figure 1. Examples of photos from the set used in this study, each with a prominent object in the foreground.

Figure 2. Examples of the three background conditions tested. (a) unattenuated, (b) darkened, (c) low-pass.

heighten the contrast with the object. Additionally, a darkened background would be expected to produce less contrast reduction from ocular stray light than a white or grey one as used in previous studies.[18,21] Lowering the mean luminance of the background, reduces its zero-frequency component. This reduces the amplitudes of the higher frequency components while leaving their contrasts intact. This differs from the way in which high-pass filtering is usually applied to images, in which the mean level is subtracted before the filtering and added back in afterwards, thus introducing a frequency dependent attenuation of contrast.

This selective filtering was performed by first segmenting manually the image into object and background images, using the GIMP software under linux (Red Hat 9) on a PC computer (HP Workstation ×4000, dual processor). Then, the luminance of the background image was attenuated by 80%, after which this modified background was recombined with the unmodified object image. Image processing was performed using Matlab 6.5 (The MathWorks; http://www.mathworks.com).

For 15 of the 40 images, the mean luminance of the object was lower than that of the background in the original image. After darkening, the background luminance was lower than that of the object in all 40 images. In other words, the darkened background reversed the figure/ground luminance contrast in these cases.

The 80 images [40 original (O) and 40 darkened (D)], were divided among 4 sets of 20 images (10 O/10 D) so that each individual saw 20 different images, half of each type. Whether an individual saw an image of a particular object as O or D was randomized across observers to ensure that differences in intrinsic difficulty between images would not bias the results. For each of the 80 images, a series of 9 progressively low-pass (Gaussian) filtered images was generated. Bandwidth of the images was defined as the spatial frequency at which the filter's transfer function drops to e^{-1}. Thus, for each image of an object, we created a 10 image sequence of bandwidths ranging from 4 to 64 cpi in half octave steps plus the full bandwidth image. Example sequences for unattenuated and darkened background images are shown in the top two rows of *Figure 3*.

In the second experiment, observers were tested in central and peripheral vision at 5.5° eccentricity. For the size stimuli that we used, only an extreme edge of the image crossed the fovea at this eccentricity. This eccentricity was chosen based on the average distance of the nearest healthy patch of retina in our patient sample, based on

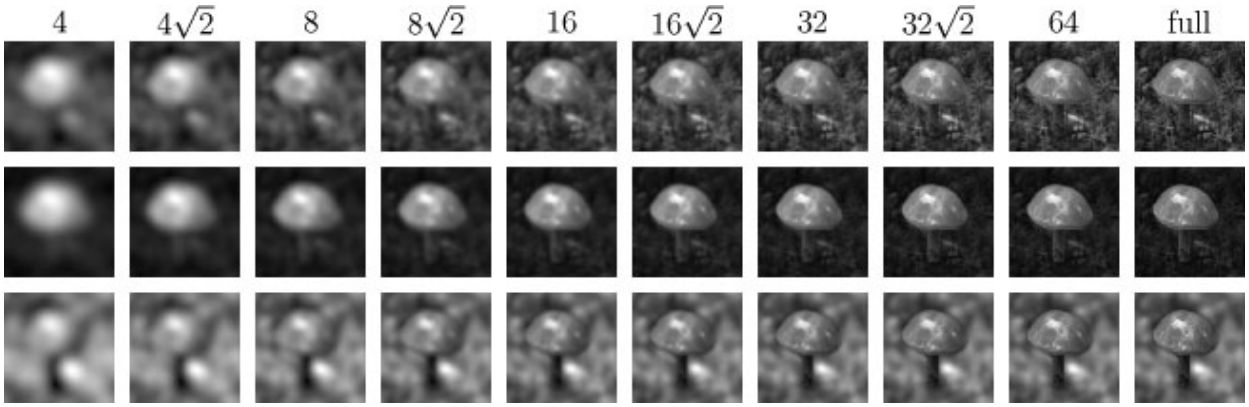

Figure 3. Top, bandwidth in cycles/image. First row image sequence, 10 bandwidths of images with an unattenuated background. Second row, 10 bandwidths of images with a darkened background. Bottom image sequence, 10 bandwidths of images with a low-pass background. Given the resolution of the images, the full bandwidth condition is equivalent to a bandwidth of 128 cpi.

Goldmann dynamic perimetry. Three background conditions were tested, unattenuated (original image) and two types of background attenuation. The background attenuation could be darkened as in the first experiment or low-pass filtered (L) (*Figure 2c*). The background attenuation was performed in a similar fashion as described above for the darkened condition. The low-pass background was obtained by filtering with a 2D isotropic Gaussian of bandwidth 8 cpi.

A set of 60 images was filtered with both methods and sets of 60 images (20O/20D/20L) were created so that each observer was presented with images of 60 different objects but the background condition of each object was randomized across observers. For each image and background, a series of progressively low-pass filtered images was generated as in the first experiment. An example bandwidth sequence for the low-pass background condition is also shown in *Figure 3* in the bottom row.

Procedures

Each image presented was square, 11 cm on a side. The observer was placed 57 cm from the display in an otherwise dark room. At this distance, one side subtended 5.5°. The background luminance of the screen was set at 65 cd m^{-2} with CIE 1931 *xy* chromaticity coordinates (0.29, 0.30). AMD was always binocular in the selected sample of patients but testing was monocular, using the eye with best acuity. Each bandwidth series, including the full-bandwidth image was presented in an ascending method of limits. For both experiments, the instructions were to identify the image as early in the series as possible. If the response was judged correct, the sequence was terminated and a sequence with a new image begun. A response was judged correct if the object was correctly named, for example, 'bateau à voiles' for sailboat and not just 'bateau' (boat). The only case in which multiple names arose is with the photo of the deer (*Figure 1a*) for which the words 'biche', 'faon' or 'daim', all common terms to describe a deer, were accepted as correct.

In Experiment 1, patients and controls (both young and elderly) were allowed to view images for unlimited duration with uncontrolled fixation. Twenty series, 10 each of natural and darkened background images, were presented in random order.

In Experiment 2, display time and fixation were controlled. The sequence of events for central and peripheral viewing is shown in *Figure 4*. A fixation target composed of a cross in a circle was displayed. At 400 ms the exterior circle disappeared. Ten milliseconds later the fixation cross disappeared, and an image appeared for 150 ms. In the central viewing condition, the image was centered at the fixation cross position. With peripheral viewing, the image appeared randomly above or below the fixation position at 5.5° eccentricity. The duration of the stimulus was sufficiently short to preclude the programming of a saccade to change fixation.

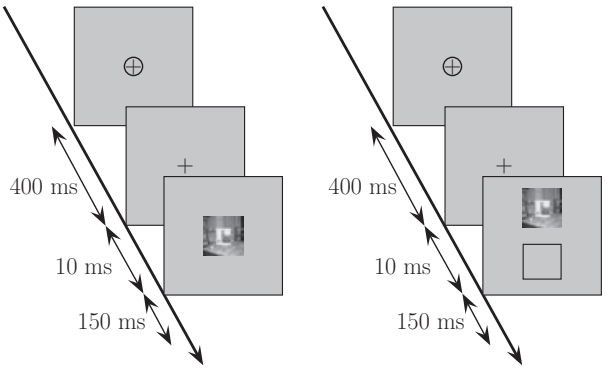

Figure 4. Stimulus sequence of Experiment 2. Left, central presentation; right, peripheral presentation (superior or inferior). The square box in the lower visual field in the right image is virtual and was not present in the actual experiment.

During a session of Experiment 2, images of all 60 objects were presented to the observer, 20 with an unattenuated background, 20 with a darkened background and 20 with a low-pass background. As in the first experiment, the image subsets, background condition and eccentricity were counterbalanced across observers. The session was divided into four sub-sessions with 15 image sequences in each. The sub-sessions contained five sequences from each background condition and were assigned to foveal and peripheral viewing in an ABBA design to control for effects of learning and fatigue. An entire session lasted between 30 and 45 min.

Results

Experiment 1

The results were analyzed first by fitting a psychometric function to the proportion of images identified as a function of bandwidth. This approach collapses the data across images (but not condition) and allows estimation of critical features, such as the critical bandwidth, bw_c, defined here as the bandwidth at which 50% of the images were recognized and the proportion of unrecognized images at full bandwidth. To take into account possible effects due to the images selected (item effects) and their contrast, we also, performed analyses of the minimal bandwidth at which each image was recognized, $bw_{\min}$.

Critical bandwidth and proportion unrecognized.

For each condition, the number of images correctly identified was tabulated at each bandwidth tested. In general, the proportion of images recognized increases with

increasing bandwidth. Thus, this method of analysis yields a psychometric function indicating the cumulative number of correctly identified images as a function of bandwidth. The characteristics of the data were then summarized by the parameters obtained after fitting an analytic function using a maximum likelihood criterion.[36,37] For this purpose, we used a Weibull function parameterized so that the critical bandwidth, as we have defined it, was an explicitly estimated parameter,

$$P(bw) = (1-\delta)\left(1 - e^{-\ln\left(\frac{2-2\delta}{1-2\delta}\right)\left(\frac{bw}{bw_c}\right)^{\beta}}\right), \qquad (3)$$

where bw is the bandwidth in cpi, bw_c the critical bandwidth defined as the bandwidth at which 50% of the images were recognized, β a steepness parameter, and δ the proportion of unrecognized images at full bandwidth. By taking the logarithmic term out of the exponent, this expression can be simplified to,

$$P(bw) = (1-\delta)\left(1 - \left(\frac{1-2\delta}{2-2\delta}\right)^{\left(\frac{bw}{bw_c}\right)^{\beta}}\right). \qquad (4)$$

Example data from one observer from the AMD group for two conditions with the fitted equations are shown in *Figure 5*. We analyzed two parameters from the fitted function, the critical bandwidth for image recognition, bw_c, and the proportion of unrecognized images at full bandwidth, δ. Note that our definition of critical bandwidth is with respect to the absolute number of image sequences presented – the right side of *Equation 4* equals 0.5 when $bw = bw_c$ – and not with respect to the upper asymptote of the psychometric function, as would be the case if the parameter δ did not figure in the argument of the exponential in *Equation 3*. Given the large individual differences in the upper asymptotes observed for the AMD observers, it would be difficult to compare and interpret the critical bandwidths defined in terms of a criterion point on the psychometric function, itself.

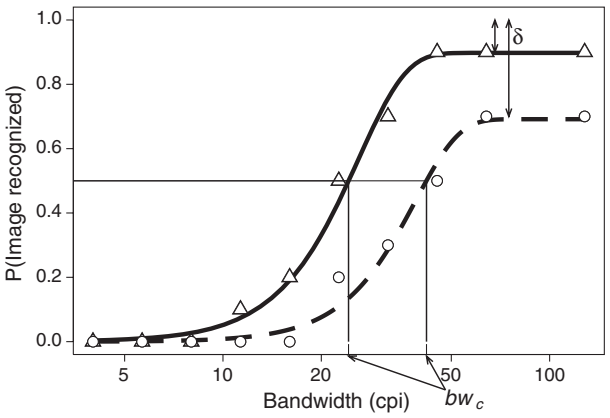

Figure 5. Proportion of images recognized as a function of bandwidth for one observer. The circles were obtained from images with unattenuated backgrounds and the triangles for darkened backgrounds. The solid and dashed curves indicate the maximum likelihood fits of *Equation 3* to each data set. The critical bandwidth, bw_c is defined as the bandwidth at which 50% of the images are recognized. The upper asymptote is parameterized by δ, the proportion of images not recognized at full bandwidth.

To homogenize variance, a log transformation was applied to the bw_c estimates and a cube-root transformation to δ in subsequent statistical analyses, suggested by a Box–Cox transformation[38] and verified in subsequent diagnostic plots of the fitted models. In some cases, a patient recognized <50% of the images at full bandwidth, which resulted in infinite estimates for bw_c (the argument of the logarithm becomes negative). We describe how we treated these cases below. All fits and statistical analyses were performed in the R statistical computing environment.[39]

Figure 6a shows the average bw_c and standard errors for the unattenuated and darkened background images for each of the three groups tested. The data were analyzed with a linear mixed-effects model in which subject was treated as a random factor and type of background was nested within group.[40] A significant bandwidth difference was associated with the main effect of groups ($F_{2,37} = 59.9$, $p < 0.0001$) and with the type of background within each group ($F_{3,37} = 9.66$, $p < 0.0001$). Young normal observers required a lower bw_c for image recognition than older normal observers ($t_{37} = -4.61$, $p < 0.0001$) who in turn required a lower bw_c than the AMD group ($t_{37} = -7.93$, $p < 0.0001$). For all three groups, the images with darkened backgrounds were recognized at a lower bw_c than those with unattenuated backgrounds (young: $t_{37} = -2.4$, $p = 0.02$; older: $t_{37} = -2.45$, $p = 0.02$; AMD: $t_{37} = -4.16$, $p = 0.0002$).

For seven observers from the AMD group, the upper asymptote was <50% for at least one image type. In these cases bw_c becomes infinite and is technically undefined. The means and the analyses for the AMD group in *Figure 6a* are from the seven observers who recognized more than 50% of both types of images. The AMD data, re-analyzed for all observers using a Wilcoxon signed rank test with the undefined bw_c values assigned to infinity, still reveal a significant decrease in critical bandwidth for images with a darkened background ($T = 64$, $p < 0.01$) as, also, do the groups with a normal visual field, when analyzed with this test (young: $T = 80$, $p = 0.01$; older: $T = 153$, $p = 0.03$).

Figure 6b shows the average values of δ and standard errors for the unattenuated and darkened background

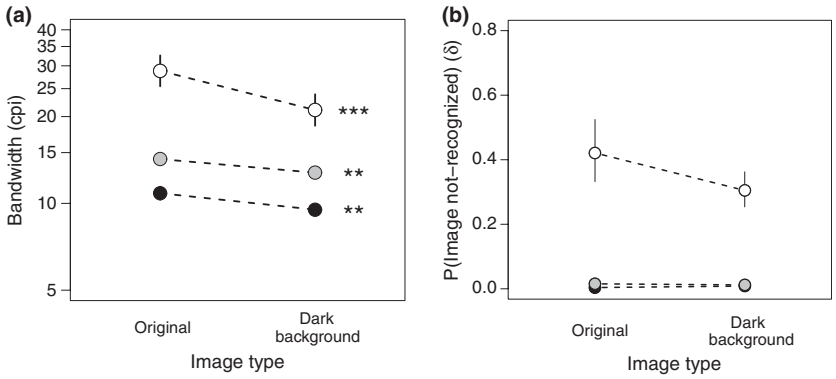

Figure 6. (a) Average critical bandwidth for original images with an unattenuated background and for images with a darkened background. The error bars here and in subsequent images are standard errors. If not shown, then they are smaller than the symbols. The black circles are for the young group, the grey symbols the older group and the white symbols the AMD group. (b) Proportion of images not recognized at full bandwidth for both types of images. Note that the error bars are asymmetric. The data were analyzed on a cube root scale but have been transformed back to their original scale to facilitate interpretation. Color scheme is the same as in adjacent figure (*$p < 0.05$, **$p < 0.01$, ***$p < 0.001$).

conditions for each experimental group. These data were analyzed with the same model used to test bw_c but with the cube root of δ the response variable. A significant difference was found for the main effect of groups ($F_{2,44} = 77.3$, $p < 0.0001$) due to the difference between the AMD and older groups ($t_{44} = 10.61$, $p < 0.0001$). The difference between the young and older groups attained significance, as well, ($t_{44} = 1.78$, $p = 0.04$), even though the differences are much smaller.

The main effect of background type within group was not significant ($F_{3,44} = 1.88$, $p = 0.66$) even though a greater number of darkened background images were recognized at full bandwidth by the AMD group. No significant asymptote differences were obtained between background types for the young and older groups, however (young: $t_{44} = 1.16$, $p = 0.13$; old: $t_{44} = -0.06$, $p = 0.73$).

Similar to the report by Mazoyer *et al.*,[18] AMD observers require a lower bw_c to recognize images when the background is attenuated. Here, we find a tendency to recognize more images at full bandwidth on a darkened background, though not a significant one. Young and older observers with normal central fields also require a lower bw_c to recognize background-attenuated images, but the effect is smaller. In general, both of these groups require less bandwidth overall than the AMD observers with the young group outperforming the older group.

The bw_c improvement in the AMD group is interesting, also, because none of the other covariates or factors in *Table 1* account for bw_c and δ estimates. *Table 2* shows the statistical results of adding one additional explanatory variable (indicated in the first column) for the AMD group. None of the additional variables produce a significantly better fit of the model.

Table 2. Summary statistics for adding an explanatory variable. Summary of conditional *F*-statistics and *p*-values obtained by adding a factor or covariate from *Table 1* as an explanatory variable to model the effects of background type on critical bandwidth and proportion of images unrecognized by AMD patients

	bw_c		δ	
	F	*p*	*F*	*p*
LogMAR	0.91	0.38	0.60	0.47
Reading rate	1.03	0.35	0.32	0.59
Scotoma type	1.71	0.24	4.13	0.09
AMD type	2.83	0.14	0.67	0.44

The improvement due to background type in the AMD observers is about 35%. Given the variability among the AMD observers, this value is commensurate with the average value of 50% reported by Mazoyer *et al.*,[18] and for which the attenuated background was white instead of being darkened.

Minimal bandwidth.

In the analyses in the previous section, the results from all the images were combined to produce a psychometric function from which performance measures were estimated. Observed differences that might be due to the intrinsic difficulty of recognizing a particular image or the overall contrast of the image were, in a sense, averaged over. The randomization of images over conditions and observers would also tend to obviate the role of such factors in the results, relegating their effects to the error terms in the modeling of the data. However, if instead of the critical bandwidth, we examine the lowest bandwidth at which an image was recognized, $bw_{\min}$, then

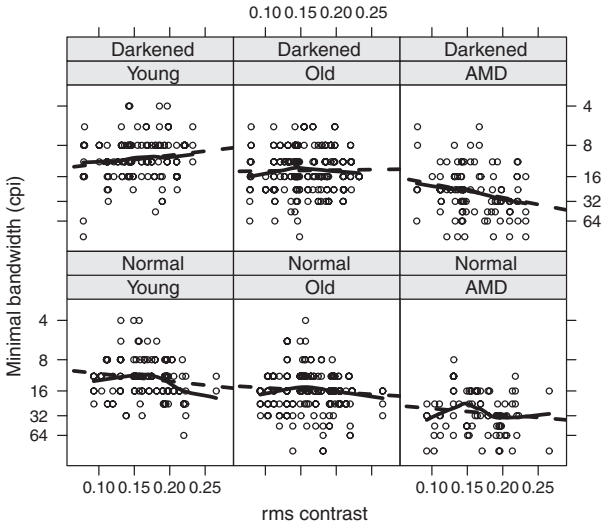

Figure 7. Minimal bandwidth for image recognition is plotted as a function of rms contrast of images for each group and background condition. The spacing on the ordinate is in terms of the inverse cube root. The solid lines represent a local regression curve fit to the points and the dashed lines are the best fitting linear regressions.

we can model such effects to determine their influence on the results.

As with the previous analyses, we evaluated the statistic under consideration with a Box–Cox transformation and found that an inverse cube root provided the best variance stabilizing transformation of the dependent variable. *Figure 7* shows the minimal bandwidths for all images and observers for each of the groups and conditions. The ordinate spacing is in terms of the inverse cube root transformation so that higher bandwidths are lower on the scale. The rms contrasts of the images vary by a factor of 3.5:1. The solid lines show a local regression curve fit to the data and the dashed lines are the best-fitting linear regression. The similarity of the two curves suggests that there are no important nonlinearities in the relation between bandwidth and image contrast. The curves suggest that AMD observers required higher values $bw_{\min}$ than younger or older normal observers on average and that a dependence of bandwidth on image contrast for the darkened images might occur for the AMD group.

We fit a series of linear mixed-effects models to describe these data. As fixed-effects, we included image background manipulation and group as two- and three-level factors, respectively, and the logarithm of the rms contrast as a covariate. Observers and images were treated as grouping factors for the random effects. We initially evaluated the random effects in a model in which all orders of interactions of the fixed-effects were retained. Using likelihood ratio tests, we found that only random intercepts associated with the grouping factors needed to be retained and that random coefficients associated with the rms contrast were unnecessary ($\chi^2_2 = 0.07$, $p = 0.97$). The variability associated with images was six times greater than that associated with observer differences. Turning to the fixed-effects, we found that the three-way interaction between group, background condition and the rms contrast was significant ($\chi^2_2 = 6.03$, $p = 0.049$) so we retain a model with all marginal terms. Examining the coefficients of the fitted model, we find a significant dependence of $bw_{\min}$ on rms contrast in the AMD group for darkened backgrounds ($t_{939} = -2.43$, $p = 0.016$). This effect corresponds to the negative slope apparent in the AMD/Darkened condition of *Figure 7*. Lower rms contrast images require a lower bandwidth for recognition when the background is darkened. An inverse effect is observed in the young group with observers requiring slightly lower bandwidths with darkened backgrounds at higher rms ($t_{939} = 2.45$, $p = 0.016$). Two other effects were significant. On average the $bw_{\min}$ was lower when the background was darkened ($t_{939} = 3.24$, $p = 0.001$) and, unsurprisingly, the AMD group required higher $bw_{\min}$ on unmodified backgrounds ($t_{939} = -11.02$, $p < 0.001$).

The results demonstrate that the bandwidth requirements for image recognition of AMD observers depend on the rms contrast of images when the background is darkened. Interestingly, however, the dependence was such that their performance improved for images of lower rms contrast. This behavior was inverse to that of young normal observers whose bandwidth requirements diminished slightly at higher rms contrast. Higher rms contrast implies greater variation in the pixels of an image but the measure gives no information on the scale of variation. Perhaps, such variation, if at the appropriate scale, could interfere with or mask object recognition in low vision observers.

Experiment 2

In the first experiment, observers with normal central visual fields showed a modest but significant decrease in critical bandwidth for recognition of images with a darkened background while AMD observers displayed a larger but contrast dependent effect. The central scotoma of the AMD observers obliges them to process images in their peripheral visual fields. It may be that characteristics specific to peripheral vision exaggerate the difficulty of separating figure from ground. While the lack of correlation between the preceding results and patient acuity argues against peripheral resolution losses[22] as the limiting factor, other factors cannot be excluded. If the bandwidth advantage for background attenuated images is due to characteristics of the peripheral visual field, then we

would expect that normal observers, also, would display a larger bandwidth advantage in the periphery for images with an attenuated background. This hypothesis was evaluated on a group of young observers, tested in the fovea and at 5.5° eccentricity and with two methods of background attenuation. In addition to the darkened background images, a low-pass filtered background was used. This condition was motivated by the report of Webster *et al.*[41] that low-pass backgrounds make objects appear sharper, as if their high frequency spectra were amplified. Indeed, observers sometimes remarked that the full bandwidth object on a low-pass background, as in *Figure 2c*, seems to stand out in depth.

Figure 8a shows the average bw_c for foveal and peripheral presentation for each of the background conditions. The white symbols indicate the images with an unattenuated background, the gray the low-pass background and the black the darkened background. The data were analyzed with a linear mixed-effects model[40] in which the factors type of background attenuation and eccentricity were crossed fixed effects and observer was a random factor. As before, the Box–Cox transformation indicated that we analyze the logarithm of the dependent variable.

The effect of background attenuation was significant ($F_{2,45} = 7.83$, $p = 0.001$). This is due to the darkened background images in the fovea ($t_{45} = 2.15$, $p = 0.04$) and the periphery ($t_{45} = 3.35$, $p = 0.002$), the low-pass background providing a just significant bandwidth advantage only in the periphery ($t_{45} = 2.02$, $p = 0.049$). The effect of eccentricity was not significant ($F_{1,45} = 0.15$, $p = 0.70$), nor was the interaction with background type (Back×Ecc: $F_{2,45} = 1.26$, $p = 0.29$).

Figure 8b indicates the values of δ for central and peripheral viewing for the three background conditions. The symbols refer to the same conditions as in the adjacent figure. Preliminary analyses showed the distribution of these data to be highly skewed (*Figure 9*), which would invalidate the normality assumption in a linear mixed-effects model. Even though the Box–Cox transformation indicated that a logarithmic transformation would be appropriate for these data, we opted for a more conservative approach by analyzing the data with a distribution-free permutation test.[42,43] The null hypothesis under which the permutations are generated is that the δ's from all six conditions arise from the same distribution. From the original data, 200 permutations of these six values were generated for each observer. Comparisons (contrasts) of interest were calculated on the permuted sets from each observer (e.g., Foveal vs Peripheral presentation), which were then averaged across observers. The significance level of a contrast was determined by the proportion of times the average values from the permuted sets were greater than the value from the original set. The sampling schema that we used preserves the within-subject design of the experiment.

The data show an effect of eccentricity ($p = 0.006$) which seems to be due to differential effects of background attenuation in the periphery. The effects of background type within eccentricity are significant in the periphery for the comparison of the low-pass with the unattenuated background ($p = 0.004$) and marginally so for the comparison of darkened with the unattenuated background in the periphery ($p = 0.049$). Neither of the comparisons for foveal presentation were significant (unattenuated/darkened $p = 0.36$, unattenuated/low-pass $p = 0.52$).

Discussion

We observed a reduction in the bandwidth necessary for image identification in AMD observers when the background was attenuated by lowering its luminance. The improvement is unlikely to be due to an effect of memory as none of the images were repeated for a given observer.

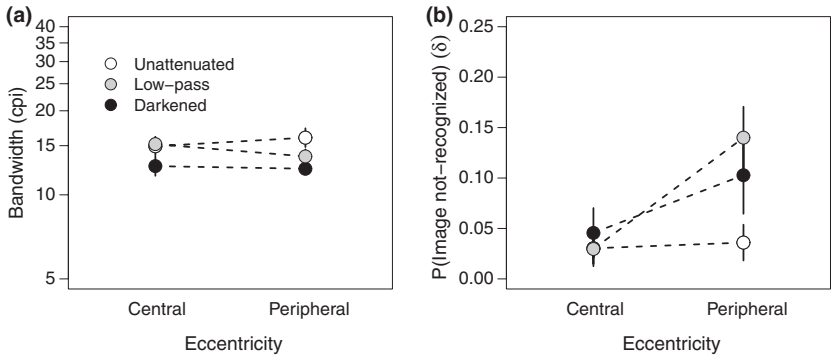

Figure 8. (a) Average critical bandwidth for image recognition in central and peripheral (5.5°) viewing. The white circles correspond to an unattenuated background, the grey circles a low-pass background and the black circles a darkened background. (b) Proportion of images not recognized at full bandwidth for central and peripheral viewing. The color scheme is the same as in the adjacent figure.

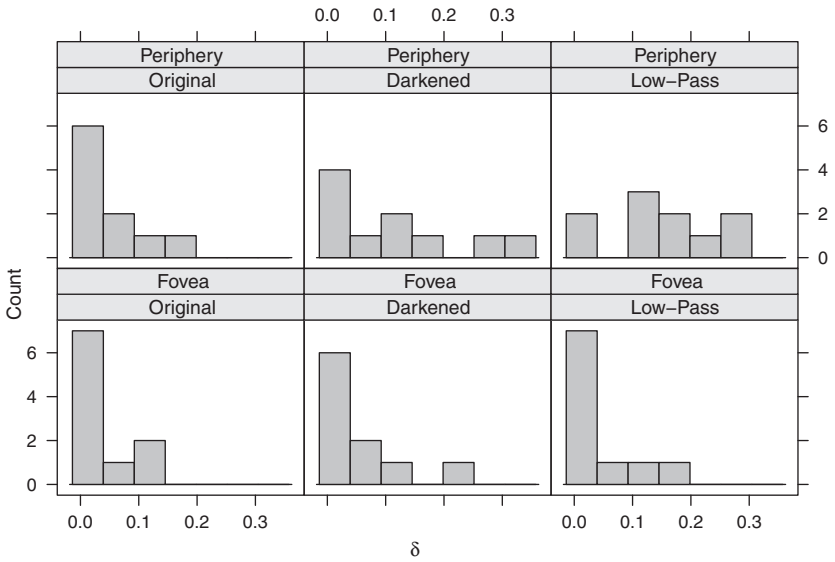

Figure 9. Histograms of the fitted parameter δ, the proportion of images unrecognized, for each of three background conditions and eccentricity.

In a previous study in which observers were tested with both novel and repeated images over several sessions, no reduction in critical bandwidth was reported for the novel images while a reduction was found for the repeated ones.[44] This suggests, in addition, that there would be little effect of learning. The improvement did depend on the rms contrast of the images with a trend toward greater improvement at lower rms values. An increase found in the number of images recognized at full bandwidth, however, was not significant. Observers with normal central vision showed similar but smaller bandwidth reductions. Since they recognized nearly all of the images at full bandwidth, however, no effect of the total number of images was measurable.

The bandwidth of an image was defined by the half-width at a criterion height of the Gaussian filter with which the image was convolved. Different images, however, are not necessarily of equivalent difficulty and may require more or less bandwidth for recognition. By counterbalancing the images and the conditions across observers, such differences would tend to average out. Counter-balancing in this way controls for potential differences in intrinsic difficulty of images between conditions, a factor not explicitly controlled in previous studies.

In addition, however, we also analyzed the minimal bandwidth at which individual images were recognized. This allowed us to include the images as a random item effect and also to examine specific image characteristics, here the rms contrast, as covariates. When this was done, we observed that the observed improvement depended on the rms contrast of the images in AMD but not in the normal, aged group of observers. The young group also showed a small contrast effect for images on darkened backgrounds but it was in the opposite direction of AMD observers with a small decrease in minimal bandwidth with increased contrast. This result, then, concurs with a previous study in which a significant correlation between contrast sensitivity and critical bandwidth was observed.[18]

Interestingly, the bandwidth improvements in the AMD patients were not correlated with other measures of visual function, such as visual acuity, reading rate, etc. It is tempting to speculate that critical bandwidth for image recognition, like that for letter recognition,[31] reading,[3,32] face recognition[33,34] and recognition of simple 3D geometric objects,[35] should be related, at least in part, to a stage of object processing, rather than of just spatial stimulus encoding.

In this study, young observers with a normal central visual field required about 12 cpi for recognition of freely viewed images with an unattenuated background. This value was reduced to about 9.5 cpi when the background was darkened. These values are similar to the bandwidths required for face recognition[33,34] which have been reported to range from 6 to 16 cycles/face but are greater than those for recognition of simple 3D geometric shapes[35] which are near 4 cycles/object. Letters, on the other hand, require only an octave above their fundamental frequency for identification.[31] The higher bandwidth requirements for object recognition may reflect the greater complexity of the images as well as the larger choice in the number of responses for this type of task.

The hypothesis that performance in the normal periphery would be similar to that of AMD observers was not

supported. Not only were the bandwidth effects equivalent or less than those in the fovea, but fewer images were recognized at full bandwidth for the background attenuated images, which is the reverse of what was observed in AMD. One could argue that if the images were presented even more eccentrically, we might have observed effects similar to those in AMD. For this to be true, the bandwidth requirements for recognizing the images with an unattenuated background would have to increase more rapidly than for attenuated background images so as to reverse the current trends. It should be noted that the normal observers reported that at the eccentricities examined, the task was already quite difficult.

Another difference between the first and second experiments is the short stimulus durations necessary to control the eccentricity of presentation. The observers of the first experiment were permitted unlimited viewing and uncontrolled fixation. These conditions were not sufficient, however, to enable some AMD observers to identify every image at full bandwidth. In contrast, at short durations, only in the periphery were normal observers unable to recognize all images at full bandwidth. Short durations were used to prevent observers from making a saccadic eye movement during stimulus presentation. Optimal durations for recognition, however, depend on several factors including task complexity, age and retinal eccentricity.[45–49] It is likely that with longer stimulus durations more images would be recognized in the periphery. While eccentricity dependent temporal processing differences render it problematic to compare foveal and peripheral results, they do not invalidate comparisons of the different background conditions within eccentricity.

A recent study found shorter reaction times and a higher percentage of isolated images recognized in AMD observers with fixed, short-duration displays.[21] Thus, it does not seem likely that the selective improvement observed for images with an attenuated background for AMD observers compared to the results from the normal periphery can be explained by the longer exploration time available to them. An alternative explanation could require positing a reorganization of the visual mechanisms in their peripheral visual fields such as has been recently proposed to explain differences in foveal and peripheral grating summation in aging.[50] Note, however, that AMD observers performed more poorly than normal observers under all conditions, possibly indicating evidence of pathology in the periphery or less efficient use of peripheral vision.[48,51]

To our surprise, the performance on the low-pass backgrounds was inferior to that for darkened or unattenuated backgrounds in that fewer images were recognized at full bandwidth in the normal periphery, although they were recognized at slightly lower bandwidth. Perhaps, the bandwidth of the background was too high so that it was not sufficiently different from that of the object in the image. Lowering the background bandwidth would bring it closer to a condition of a gray background at the mean luminance. The inferiority of this condition suggests that the benefits accrued from the darkened and white background conditions[18] are due to the heightened contrast generated between the figure and ground in these images. This does not mean that it is sufficient to increase the contrast globally in an image to render it more recognizable for low vision observers, since doing so will affect both the figure and the ground and, in fact, seems possibly to interfere with the bandwidth requirements here. On the contrary, our results suggest that selective increase of the contrast of the object in the image with respect to the background renders these images easier to identify by observers with AMD. In order for such methods to be implemented, it will require image processing techniques that are capable of pre-segmenting an object from the background. It would be of interest to explore whether other methods that differentially affect image foreground and background characteristics would be equally or more effective for low vision obsevers.

Unfortunately, the current state of the art in image segmentation is not sufficiently advanced to implement such an algorithm in real-time. Some progress has been made in determining what parts of an image are likely to be salient to an observer, as defined by frequency of exploration by eye movements.[52–54] However, the most salient part of an image may not necessarily contain the object of interest to an observer. In addition, how might regions be selected when multiple objects are present? It would seem that some sort of interaction with the attentional mechanisms of an observer would be necessary.[55] Issues related to partial occlusion of objects, shadow and illumination will have to be resolved, as well.

We feel that the value of our finding is in drawing attention to the possibility that processing beyond early vision may need to be incorporated into understanding the coding deficits in AMD. In addition, even if a real-time application is not currently practicable, it would still be feasible to enhance static images, as we have done, meant for low vision observers, e.g., for brochures or large print books. Finally, it is possible that even though the improvements that we observe seem modest, they could be quite significant for an observer with impaired vision.

Acknowledgements

Supported by grants from INSERM, the Région Rhône-Alpes (Émergence) and the European Union, AMD-READ (QLK6-CT-2002-00214). Gary Rubin is thanked for helpful comments and criticisms of an earlier version.

References

1. Coscas G. Dégénérescences Maculaires Acquises Liées à l'Age et Néovaisseaux Sous-rétiniens. Masson: Paris, 1991.
2. Kupfer C. The National Eye Institute's low vision education program improving quality of life. *Ophthalmology* 2000; 107: 229–230.
3. Legge GE, Rubin GS, Pelli D & Schleske MM. Psychophysics of reading–II. Low vision. *Vision Res* 1985; 25: 253–265.
4. Wang YZ, Wilson E, Locke KG & Edwards AO. Shape discrimination in age-related macular degeneration. *Invest Ophthalmol Vis Sci* 2002; 43: 2055–2062.
5. Lord SR. Visual risk factors for falls in older people. *Age Ageing* 2006; 35 (Suppl 2): ii42–ii45.
6. Soubrane G, Coscas G, Francais C & Koenig F. Occult subretinal new vessels in agerelated macular degeneration: natural history and early laser treatment. *Ophthalmology* 1990; 97: 649–657.
7. Stokkermans TJW. Treatment of age-related macular degeneration. *Clin Eye Vis Care* 2000; 12: 15–35.
8. Park W. Vision rehabilitation for age-related macular degeneration. *Int Ophthalmol Clin* 1999; 39: 143–162.
9. Brown MM, Brown GC, Sharma S, Landy J & Bakal J. Quality of life with visual acuity loss from diabetic retinopathy and age-related macular degeneration. *Arch Ophthalmol* 2002; 120: 481–484.
10. Massof R & Rickman D. Obstacles encountered in the development of the low vision enhancement system. *Optom Vis Sci* 1992; 69: 32–41.
11. Pelli DG, Legge GE & Schleske MM. Psychophysics of reading. III. A fiberscope low vision reading aid. *Invest Ophthalmol Vis Sci* 1985; 26: 751–763.
12. Vettard S, Dubois E, Quaranta M & Mauget-Faysse M. Prismatic treatment in low vision rehabilitation of patients with age-related macular degeneration. *J Fr Ophtalmol* 2004; 27: 589–596.
13. Peli E, Kim J, Yitzhaky Y, Goldstein RB & Woods RL. Wideband enhancement of television images for people with visual impairments. *J Opt Soc Am A Opt Image Sci Vis* 2004; 21: 937–950.
14. Nilsson UL, Frennesson C & Nilsson SE. Patients with AMD and a large absolute central scotoma can be trained successfully to use eccentric viewing, as demonstrated in a scanning laser ophthalmoscope. *Vision Res* 2003; 43: 1777–1787.
15. Crossland MD, Culham LE, Kabanarou SA & Rubin GS. Preferred retinal locus development in patients with macular disease. *Ophthalmology* 2005; 112: 1579–1585.
16. Lawton TA, Sebag J, Sadun AA & Castleman KR. Image enhancement improves reading performance in age-related macular degeneration patients. *Vision Res* 1998; 38: 153–162.
17. Knoblauch K, Mazoyer V, Koenig F & Vital-Durand F. Facilitated visual search at low color contrast. *Color Res Appl* 2001; 26: S157–S160.
18. Mazoyer V, Knoblauch K, Fontanay S, Koenig F & Vital-Durand F. Identification of low-pass filtered images by low vision patients. *Vis Impair Res* 1999; I: 187–192.
19. Turano KA, Geruschat DR & Baker FH. Fixation behavior while walking: persons with central visual field loss. *Vision Res* 2002; 42: 2635–2644.
20. Stelmack JA, Tang XC, Reda DJ et al. Outcomes of the Veterans Affairs Low Vision Intervention Trial (LOVIT). *Arch Ophthalmol* 2008; 126: 608–617.
21. Boucart M, Despretz P, Hladiuk K & Desmettre T. Does context or color improve object recognition in patients with low vision? *Vis Neurosci* 2008; 25: 685–691.
22. Mandelbaum J & Sloan LL. Peripheral visual acuity. *Am J Ophthalmol* 1947; 30: 581–588.
23. Flom MC, Heath GG & Takahashi E. Contour interaction and visual resolution: Contralateral effects. *Science* 1963; 142: 979–980.
24. Bouma H. Interaction effects in parafoveal letter recognition. *Nature* 1970; 226: 177–178.
25. Levi DM, Klein SA & Aitsebaomo AP. Vernier acuity, crowding and cortical magnification. *Vision Res* 1985; 25: 963–977.
26. Peli E & Woods RL. Image enhancement for impaired vision: The challenge of evaluation. *Int J Artif Intell Tools* 2009; 18: 415–438.
27. Tu Z, Chen X, Yuille AL & Zhu SC. Image parsing; Unifying segmentation, detection and recognition. *Proc Ninth IEEE Int Conf Comput Vis (ICCV 2003)* 2003; 1: 18–25.
28. Bordier C, Koenig-Supiot F, Vital-Durand F & Knoblauch K. Image processing to facilitate image identification by partially-sighted. In: Vision 2005, International Congress Series, Vol. 1282. Elsevier: Oxford, 2005; pp. 980–984.
29. Bryant RC, Seibel EJ, Lee CM & Schroder KE. Low-cost wearable low-vision aid using a handmade retinal light-scanning microdisplay. *J Soc Inf Disp* 2004; 12: 397–404.
30. Everingham MR, Thomas BT & Troscianko T. Wearable mobility aid for low vision using scene classification in a Markov random field model framework. *Int J Hum Comput Interact* 2003; 15: 231–244.
31. Solomon JA & Pelli DG. The visual filter mediating letter identification. *Nature* 1994; 369: 395–397.
32. Legge GE, Rubin GS, Pelli D & Schleske MM. Psychophysics of reading–I. Normal vision. *Vision Res* 1985; 25: 239–252.
33. Costen NP, Parker D & Craw I. Effects of high-pass and low-pass spatial filtering on face identification. *Percept Psychophys* 1996; 58: 602–612.
34. Nasanen R. Spatial frequency bandwidth used in the recognition of facial images. *Vision Res* 1999; 39: 3824–3833.
35. Braje WL, Tjan BS & Legge GE. Human efficiency for recognizing and detecting low pass filtered objects. *Vision Res* 1995; 35: 2955–2966.
36. Watson AB. Probability summation over time. *Vision Res* 1979; 19: 515–522.
37. Yssaad-Fesselier R & Knoblauch K. Modeling psychometric functions in R. *Behav Res Methods* 2006; 38: 28–41.

38. Venables WN & Ripley BD. *Modern Applied Statistics with S*, 4th edn. Springer: New York, 2002.
39. R Development Core Team. R: A Language and Environment for Statistical Computing. R Foundation for Statistical Computing: Vienna, Austria, 2010. URL http://www.R-project.org ISBN 3-900051-00-3.
40. Pinheiro JC & Bates DM. *Mixed-Effects Models in S and S-PLUS*. Springer: New York, 2000; pp. 57–96.
41. Webster MA & Georgeson MA, Webster SM. Neural adjustment to image blur. *Nat Neurosci* 2002; 5: 839–840.
42. Efron B & Tibshirani RJ. *An Introduction to the Bootstrap*. Chapman & Hall: New York, 1993; pp. 202–219.
43. Manly BFJ. *Randomization, Bootstrap and Monte Carlo Methods in Biology*, 2nd edn. Chapman & Hall: London, 1997; pp. 125–141.
44. Mazoyer V, Knoblauch K, Koenig F & Vital-Durand F. Memory and learning in identification of low-pass-filtered images by low vision patients. *Perception* 1998; 27 (Suppl): 156.
45. Baron WS & Westheimer G. Visual acuity as a function of exposure duration. *J Opt Soc Am* 1973; 63: 212–219.
46. Rubin GS & Turano K. Reading without saccadic eye movements. *Vision Res* 1992; 32: 895–902.
47. Seiple W, Holopigian K, Shnayder Y & Szlyk JP. Duration thresholds for target detection and identification in the peripheral visual field. *Optom Vis Sci* 2001; 78: 169–176.
48. Cheong AM, Legge GE, Lawrence MG, Cheung SH & Ruff MA. Relationship between slow visual processing and reading speed in people with macular degeneration. *Vision Res* 2007; 47: 2943–2955.
49. Dey AK, Pachai MV, Bennett PJ & Sekuler AB. The effects of aging and stimulus duration on face identification accuracy with differing viewpoints. *J Vision* 2010; 10: 568a. URL http://www.journalofvision.org/content/10/7/568.abstract.
50. Malania M, Devinck F, Hardy JL, Delahunt PB, Knoblauch K & Werner JS. Test of senescent change in photopic spatial summation. *J Vision* 2009; 9: 1074a. URL http://journalofvision.org/9/8/1074/.
51. Rubin GS & Turano K. Low vision reading with sequential word presentation. *Vision Res* 1994; 34: 1723–1733.
52. Itti L & Koch C. A saliency-based search mechanism for overt and covert shifts of visual attention. *Vision Res* 2000; 40: 1489–1506.
53. Chauvin A, Herault J, Marendaz C & Peyrin C. Natural scene perception: visual attractors and image processing. In: *Connectionnist Models of Cognition and Perception* (Lowe W, Bullinaria J, editors), World Scientific Press: Singapore, 2002; pp. 236–245.
54. Peters RJ, Iyer A, Itti L & Koch C. Components of bottom-up gaze allocation in natural images. *Vision Res* 2005; 45: 2397–2416.
55. Srinivasan R, Thorpe S, Deng S, Lappas T & D'Zmura M. Decoding attentional orientation from EEG spectra. In: *Human-Computer Interaction, Part I, HCII 2009, LNCS 5610* (Jacko J, editor), Springer: Berlin, 2009, pp. 32–39.